LMI Based Gain Scheduled H_∞ Controller Design for AMB Systems under Gyroscopic and Unbalance Disturbance Effect

Selim Sivrioglu and Kenzo Nonami
Department of Mechanical Engineering,
Faculty of Engineering, Chiba University,
1-33 Yayoi-cho,Inage-ku, Chiba 263, JAPAN

Abstract

Ultra high speed rotation in Active Magnetic Bearing (AMB) systems with their comlex structure requires powerful control system design approaches for robust stability and robust performance. Recent studies in robust control theory have offered comprehensive gain-scheduled control design approaches such as Linear Matrix Inequality (LMI) based gain-scheduled control for Linear Parameter Varying Systems (LPVS) which are a certain class of linear time-varying systems that state-space matrices of their plants are fixed function of time-varying physical parameters. Rotor systems modelled with inclusion of gyroscopic effect can be considered LPV system because of affine dependence of system natural frequencies to rotational speed which is taken as time-varying parameter. These varying parameter values can be measured on line during control operation. In this study, commercially available and vertically designed a rotor bearing system is modelled and controlled using LMI based gain-scheduled controllers and compared with PID controllers. The results are reasonable and encouraging for future studies of AMB systems.

1 Introduction

Control system design for AMB systems is still one of the advanced and challenging topics for control engineers because of precise design requirements of their control system. The trends in AMB control system design is to use effective robust controller design approaches such as μ control, H_∞ control and other robust control approaches [1], [2], [3]. One of the recent topics in control related fields is linear matrix inequality (LMI) based control system design because of some good advantages. As an accepted reality, control system design using Lyapunov function establishes global asymptotic stability for control systems and LMI based gain-scheduled control design can be included this class of control design.
In the modelling stage of rotor bearing systems, gyroscopic effect is generally neglected for the aim of simplicity and this simplification may not be effect design very much in some cases. On the other hand, designing of certain kind of rotor bearing system requires the inclusion of gyroscopic effect for efficient control. For overhung rotors, the gyroscopic couple has a considerable influence on the dynamic behavior of the rotor. In the case of very high operating speeds of rotors, this kind of effect can not be neglected anymore.
There are not so many controller design studies in terms of gain scheduling technique for AMB systems in literature. In the study [4], gain scheduled H_∞ controllers are designed for eliminating unbalance vibration in AMB systems. The gain scheduling parameter of the study [4] is free parameter of Q parametrization theory and the resulting controller is also robust Linear Time Invariant (LTI) controller.
Linear Parameter Varying (LPV) plant definition plays a central role designing of gain scheduling control. LPV plants are described by state space equations of the form

$$\begin{aligned} \dot{x} &= A(\theta(t))x + B(\theta(t))u \\ y &= C(\theta(t))x + D(\theta(t))u \end{aligned} \tag{1}$$

where x, y and u denote state vector, measured output vector and control input, respectively. θ is a vector of time varying plant parameters and plant matrices are fixed functions of the θ. In practice, θ can be the time varying physical parameters such as velocity, damping, stifness and etc., and be given by

$$\theta_{min} \leq \theta_i(t) \leq \theta_{max} \tag{2}$$

The time varying parameter θ belongs to a parameter polytope Θ and varies with vertices $\theta_1, \theta_2, \ldots, \theta_r$ of this polytope

$$\theta \in \Theta = \left(\sum_{j=1}^{r} \alpha_j \theta_j \geq 0, \sum_{j=1}^{r} \alpha_j = 1 \right) \tag{3}$$

If the measurements of $\theta(t)$ are available in real time during control operation, the designed controllers have the same parameter dependence as the plant. The controller form is:

$$\begin{aligned} \dot{x}_k &= A_k(\theta(t))x + B_k(\theta(t))y \\ u &= C_k(\theta(t))x + D_k(\theta(t))y \end{aligned} \tag{4}$$

where y is the measurement vector and u is the control input. With the parameter measurements, this controller has a continues adjustment to the variations in the plant dynamics and maintains stability and good perfermance.

2 LMI Based Gain-Scheduled Control Formulation

LMI based gain-scheduled H_∞ control formulation given here is aimed for practial use. The theoretical formulation with proofs can be found in [5], [6] extensively.
Consider state-space representation of the plant given by

$$\begin{bmatrix} \dot{x} \\ z \\ y \end{bmatrix} = \begin{bmatrix} A & B_1 & B_2 \\ C_1 & D_{11} & D_{12} \\ C_2 & D_{21} & 0 \end{bmatrix} \begin{bmatrix} x \\ w \\ u \end{bmatrix} \tag{5}$$

where x is the state vector. z and y denote the controlled output and the measured output vectors, respectively. u is the control input and w is the disturturbance input vector. Given any proper real rational controller such that

$$\begin{bmatrix} \dot{x}_k \\ u \end{bmatrix} = \begin{bmatrix} A_k & B_k \\ C_k & D_k \end{bmatrix} \begin{bmatrix} x_k \\ y \end{bmatrix} \tag{6}$$

The closed-loop system can be obtained by

$$\begin{bmatrix} \dot{x}_{cl} \\ z \end{bmatrix} = \begin{bmatrix} A_{cl} & B_{cl} \\ C_{cl} & D_{cl} \end{bmatrix} \begin{bmatrix} x_{cl} \\ w \end{bmatrix} \tag{7}$$

Closed loop matrices $A_{cl}, B_{cl}, C_{cl}, D_{cl}$ are:

$$\begin{bmatrix} A_{cl} & B_{cl} \\ C_{cl} & D_{cl} \end{bmatrix} = \begin{bmatrix} A_0 + \overline{B}\Omega\overline{C} & B_0 + \overline{B}\Omega\overline{D}_{21} \\ C_0 + \overline{D}_{21}\Omega\overline{C} & D_{11} + \overline{D}_{12}\Omega\overline{D}_{21} \end{bmatrix} \tag{8}$$

where

$$\begin{bmatrix} A_0 & B_0 & \overline{B} \\ C_0 & D_{11} & \overline{D}_{12} \\ \overline{C} & \overline{D}_{21} & \Omega \end{bmatrix} = \left[\begin{array}{cc|c|cc} A & 0 & B_1 & 0 & B_2 \\ 0 & 0 & 0 & I_k & 0 \\ \hline C_1 & 0 & D_{11} & 0 & D_{12} \\ \hline 0 & I_k & 0 & A_k & B_k \\ C_2 & 0 & D_{21} & C_k & D_k \end{array}\right] \tag{9}$$

Note that controller matrices are collected into a single matrix Ω.
The Lyapunov function $V(x) = x^T P x, P > 0$ establishes global asymptotic stability for the closed-loop system (7). The L_2-induced norm from w to z for LTI system is bounded

$$\|z\|_2 < \gamma \|w\|_2 \tag{10}$$

Finally, there exists a positive definite Lyapunov function $V(x) = x^T P x, P > 0$ that satisfies

$$\frac{d}{dt} V(x) + z^T z - \gamma^2 w^T w < 0 \tag{11}$$

The H_∞ suboptimal control problem is equivalent to the existence of a solution to the following inequality for $X_{cl} > 0$

$$\begin{bmatrix} A_{cl}^T X_{cl} + X_{cl} A_{cl} & X_{cl} B_{cl} & C_{cl}^T \\ B_{cl}^T X_{cl} & -\gamma I & D_{cl}^T \\ C_{cl} & D_{cl} & -\gamma I \end{bmatrix} < 0 \tag{12}$$

Solution of the LMI (12) requires to find two symmetric matrices R and S such that

$$N_R^T \begin{bmatrix} AR + RA^T & RC_1^T & B_1 \\ C_1 R & -\gamma I & D_{11} \\ B_1^T & D_{11}^T & -\gamma I \end{bmatrix} N_R < 0 \tag{13}$$

$$N_S^T \begin{bmatrix} A^T S + SA & SB_1 & C_1^T \\ B_1^T S & -\gamma I & D_{11}^T \\ C_1 & D_{11} & -\gamma I \end{bmatrix} N_S < 0 \tag{14}$$

$$\begin{bmatrix} R & I \\ I & S \end{bmatrix} \geq 0 \tag{15}$$

where N_R and N_S denote bases of the null spaces of (B_2^T, D_{12}^T) and (C_2, D_{12}), respectively.
The above H_∞ control problem is valid only for LTI system and can be extended for LPV systems.
Let's consider state-space representation of LPV plant

$$\begin{bmatrix} \dot{x} \\ z \\ y \end{bmatrix} = \begin{bmatrix} A(\theta) & B_1(\theta) & B_2 \\ C_1(\theta) & D_{11}(\theta) & D_{12} \\ C_2 & D_{21} & 0 \end{bmatrix} \begin{bmatrix} x \\ w \\ u \end{bmatrix} \tag{16}$$

θ is a vector of time varying system parameters and plant matrices $A(\cdot), B_1(\cdot), C_1(\cdot)$ and $D_{11}(\cdot)$ are fixed functions of the θ. B_2, C_2, D_{12}, D_{21} matrices are independent of the parameter θ because of tractabilty reasons. Finally, the solution of H_∞ control problem for LPV system has the same form of LTI sytems as follows:

$$N_R^T \begin{bmatrix} A_i R + R A_i^T & R C_{1i}^T & B_{1i} \\ C_{1i} R & -\gamma I & D_{11i} \\ B_{1i}^T & D_{11i}^T & -\gamma I \end{bmatrix} N_R < 0 \tag{17}$$

$$N_S^T \begin{bmatrix} A_i^T S + S A_i & S B_{1i} & C_{1i}^T \\ B_{1i}^T S & -\gamma I & D_{11i}^T \\ C_{1i} & D_{11i} & -\gamma I \end{bmatrix} N_S < 0 \tag{18}$$

$$\begin{bmatrix} R & I \\ I & S \end{bmatrix} \geq 0 \tag{19}$$

where A_i, B_{1i}, C_{1i}, and D_{11i} denote the parameter values of $A(\theta), B_1(\theta), C_1(\theta)$ and $D_{11}(\theta)$ at the vertices $\theta = \theta_i$ of the parameter polytope.
The solution of inequalities (17), (18),and (19) is possible using advanced softwares such as convex optimization alghorithms. The construction of the controller matrix Ω from R and S matrices can be done by the same convex programs.

3 Modelling of Rotor Bearing System

The schematic drawing of magnetic bearing system for commercial use is given in Fig.1. The plant has a below side permenant magnetic bearing which has constant stiffness and damping effect and an upper side active magneting bearing which produces control inputs. Natural frequencies of the system are changing with rotational frequency as shown in Fig.2. This system is also under the unbalance disturbance effect of translational motions in x and y direction. Actual operational speed is 48000 rpm. The critical speed of rotor at rigid modes is about 5000 rpm and the first bending mode is at least twenty times higher than the rigid modes.

The equations of motion of physical system given in Fig.1 can be written by

$$
\begin{aligned}
&m\ddot{x}_g + c\dot{x}_g + kx_g = f_{x_u} + m_{un}\ell w_z^2 Coswt \\
&m\ddot{y}_g + c\dot{y}_g + ky_g = f_{y_u} + m_{un}\ell w_z^2 Sinwt \\
&J_r\ddot{\theta}_y + cl_b^2\dot{\theta}_y - J_a w_z\dot{\theta}_x + kl_b^2\theta_y = L_u f_{x_u} \\
&J_r\ddot{\theta}_x + cl_b^2\dot{\theta}_x + J_a w_z\dot{\theta}_y + kl_b^2\theta_x = -L_u f_{y_u}
\end{aligned} \tag{20}
$$

where w_z is rotational speed. The AMB system parameters are given in Table 1. The control forces produced by upper side active magnetic bearing in x and y directions can be expressed by

$$
\begin{bmatrix} f_{xu} \\ f_{yu} \end{bmatrix} = \begin{bmatrix} 2K_{du} & 0 & 2L_uK_{du} & 0 \\ 0 & 2K_{du} & 0 & -2L_uK_{du} \end{bmatrix} \times \begin{bmatrix} x_g \\ y_g \\ \theta_y \\ \theta_x \end{bmatrix} + \begin{bmatrix} 2K_{du} & 0 \\ 0 & 2K_{du} \end{bmatrix} \begin{bmatrix} i_{xu} \\ i_{yu} \end{bmatrix} \tag{21}
$$

Finally, the control system state space representation can be given by

$$
\begin{aligned}
\dot{x}_s &= A(\theta(t))x_s + B_1(\theta(t))w + B_2u \\
y &= Cx_s
\end{aligned} \tag{22}
$$

where $x_s$and y are the state vector and the measured output vector, respectively. u is the control input and w is the unbalance disturbance input. The output is:

$$
\begin{bmatrix} x_u \\ y_u \end{bmatrix} = \begin{bmatrix} 1 & 0 & 0 & 0 & l_u & 0 & 0 & 0 \\ 0 & 0 & 1 & 0 & 0 & 0 & -l_u & 0 \end{bmatrix} \begin{bmatrix} x_g \\ \dot{x}_g \\ y_g \\ \dot{y}_g \\ \theta_y \\ \dot{\theta}_y \\ \theta_x \\ \dot{\theta}_x \end{bmatrix} \tag{23}
$$

where x_u and y_u denote the displacement of the rotor at the upper side sensor location.

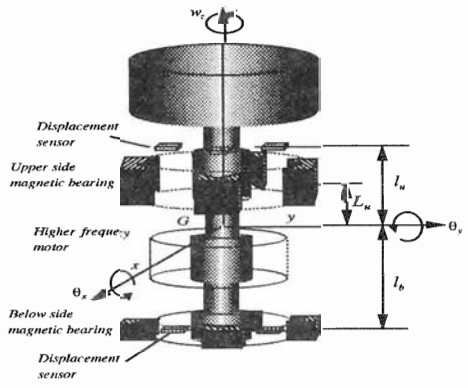

Fig.1 Vertical AMB system

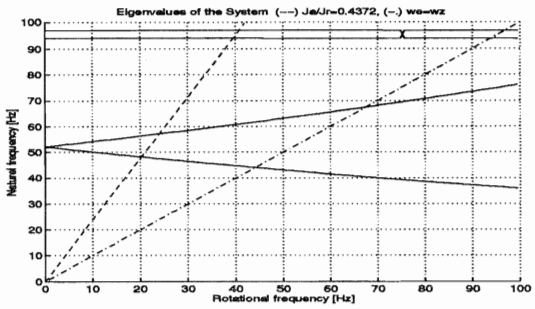

Fig.2 Natural frequencies of the system

Table 1. Parameters of AMB system

Parameter	Symbol	Value	Unit
Mass of the rotor	m	1.595	kg
Moment of inertia	J_r	0.00398	kgm^2
Polar moment of inertia	J_a	0.00174	kgm^2
Distance to C.G.	L_u	0.0128	m
Distance to C.G.	l_u	0.0314	m
Distance of sensor to C.G	l_b	0.0843	m
Upper side AMB parameter	K_{iu}	200	N/A
Upper side AMB parameter	K_{du}	3×10^5	N/m
Stiffness coefficient	k	60000	N/m
Damping coefficient	c	28.08	kg/s
Unbalance mass	m_{un}	0.0007	kg
Distance to m_{un}	ℓ	0.02	m

4 Gain Scheduled H_∞ Controller Design

Gain-scheduled control design structure of AMB system is given in Fig.3. The desired performance specifications on control system is defined in terms of frequency shaping filters W_1 and W_2. The frequency characteristics of filters is shown in Fig.4. The control system speeds up from 0 to 48000 rpm in 3 minutes and unbalance force changes with the square function of rotational speed (Fig.5). To include the unbalance as a varying disturbance input, the variation of unbalance force is linearized as shown in Fig.5(b). Parameter dependence of our system can be given by

$$
w_z \in [0, 2\pi 800] \quad rad/sec \tag{24}
$$

Specifically for this problem, the parameter vector $\theta(t)$ is:

$$
\theta(t) = \alpha_1 w_{z_{min}} + \alpha_2 w_{z_{max}}, \qquad \sum_{i=1}^{2} \alpha_i = 1 \qquad \alpha \geq 0 \tag{25}
$$

Augmented plant can be given by:

$$
G(\theta) = \begin{bmatrix} A(\theta) & B_1(\theta) & B_2 \\ C_1 & D_{11} & D_{12} \\ C_2 & D_{21} & D_{22} \end{bmatrix} \tag{26}
$$

At the corner values of θ, the plant matrix is:

$$
G(\theta) = \alpha_1 G(w_{z_{min}}) + \alpha_2 G(w_{z_{max}}) \tag{27}
$$

Finally, using the parameter dependent augmented plant, the gain-scheduled controller is computed. The structure of this controller is given by

$$
\begin{bmatrix} A_k(\theta) & B_k(\theta) \\ C_k(\theta) & D_k(\theta) \end{bmatrix} = \sum_{i=1}^{2} \alpha_i \begin{bmatrix} A_k(w_{z_i}) & B_k(w_{z_i}) \\ C_k(w_{z_i}) & D_k(w_{z_i}) \end{bmatrix} \tag{28}
$$

The simulation of above gain scheduled controller can be done for a frozen value of θ. Actually, the controller is an LTI controller at each value of parameter θ. Implementation of this controller requires the time varying parameter measurement. In our control system, using the measurement of rotational speed, the controller is continuously scheduled as shown in Fig.6.

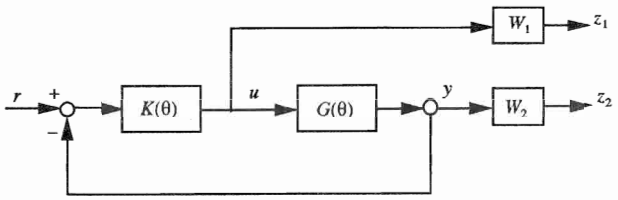

Fig.3 Control structure of the system

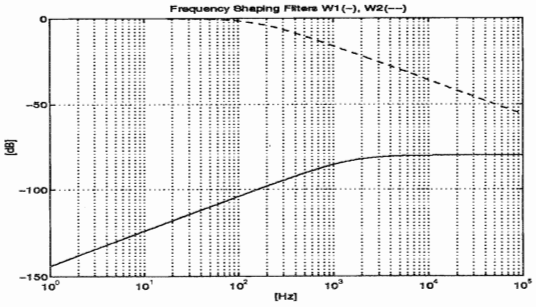

Fig.4 Frequency shaping filters

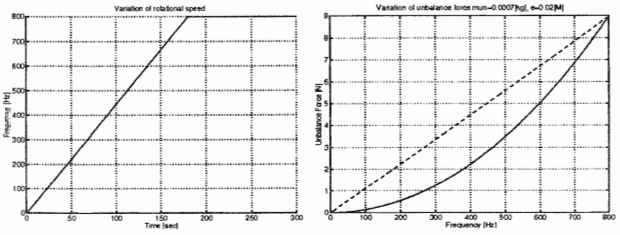

(a) (b)

Fig.5 (a) Speed up (b) Unbalance force

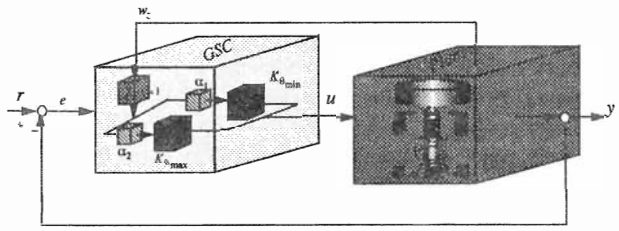

Fig.6 Gain sheduled control system

5 PID Controller

Actual PID controller is used for simulation. For each direction, the same PID controllers are operated (Fig.7). Parameters of this controller are given in Table 2. The parameters K_i and K_p are $K_i = 3$, $K_p = 0.75$. PID controller has seven filters as shown in Fig.8. The filters S_1 and S_6 are notch filters. The filters S_2, S_3 and S_4 are added for phase lead-lag action. Noise reduction is done by low-pass filter S_5. Integral action of controller is realized by S_7.

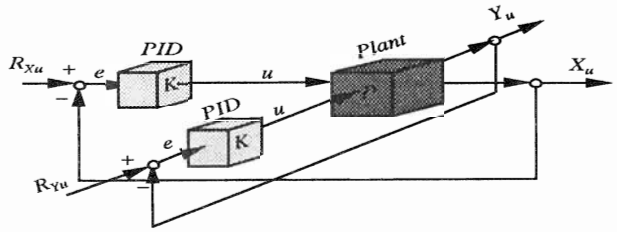

Fig.7 Control system with PID controller

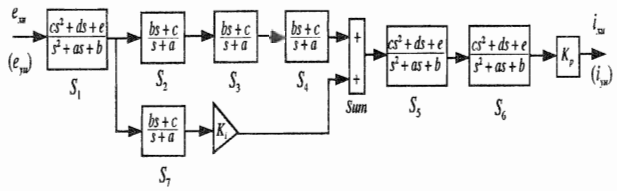

Fig.8 PID controller structure

Table 2. Parameters of PID controller

	S_1	S_2	S_3	S_4	S_5	S_6	S_7
a	7e3	200	2e4	3e4	8e3	2e3	0
b	2.1e8	2	7	7	6e7	1.25e8	0
c	1	200	2e4	3e4	0	1	1
d	0				0	0	
e	2.1e8				6e7	1.25e8	

6 Simulations

Simulation results for gain-scheduled control are obtained by using LMI Control Toolbox [7] in MATLAB. As mentioned before, control of the rotor system is done by upper side active magnetic bearing in x and y directions. The bode plots of the system is obtained from referance input R_{xu} to rotor displacement X_u at upper side sensor location and from referance input R_{xu} to rotor displacement X_b at below side sensor location.

6.1 Gain-scheduled Control Results

The bode plot of closed loop system with gain-scheduled control is given in Fig.8 and Fig.11 for both sensor locations, respectively. The results are quite acceptable for closed-loop system with gain scheduled controller. On the other hand, gain-scheduled controller showed very dynamic behaviour at certain frequency as shown in Fig.9. Comparing the closed-loop system bode plot results for both controller case, the gain-scheduled control case is better than PID case. However, gain-scheduled controller has high gain comparing with PID controller. This is not big problem for realizing the gain-scheduled controller in DSP.

The step response of closed-loop system from referance input R_{xu} to X_u is given in Fig.10. The step response with gain-scheduled control has no overshoot in this case. For below side sensor location, Fig.12 shows the step response of the closed-loop system with gain-scheduled control. For rotor-bearing system, unbalance time history response of the closed-loop system is a good measure for evaluating the controller and should obatined for both control case. The time history response given Fig.13 for gain-scheduled control case gave low amplitude rate compring with PID control.

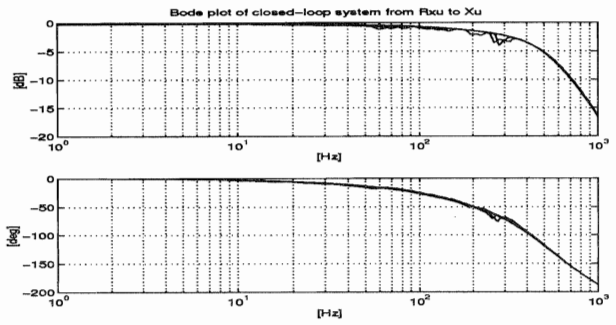

(a)

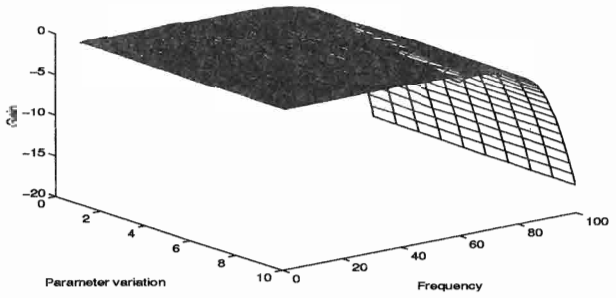

Fig.8 Bode plot of the closed-loop system with GSC
(a) 2D plot (b) 3D plot

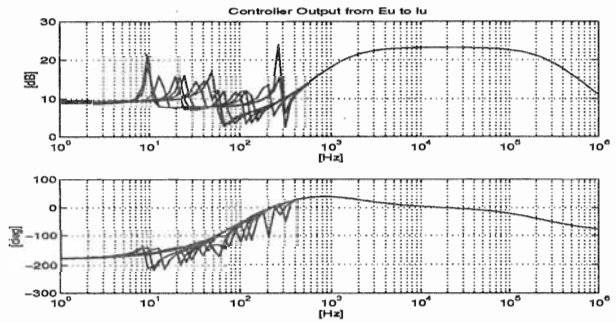

(a)

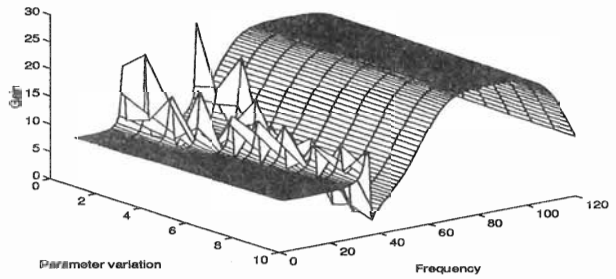

(b)

Fig.9 Bode plot of the GSC at different frequency
(a) 2D plot (b) 3D plot

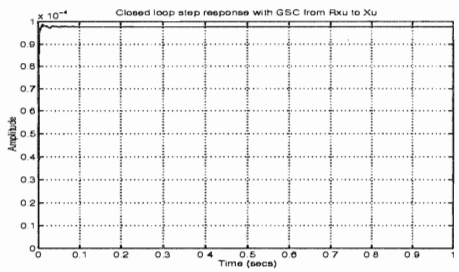

Fig.10 Step response of closed-loop system with GSC
($w_z = 100Hz$)

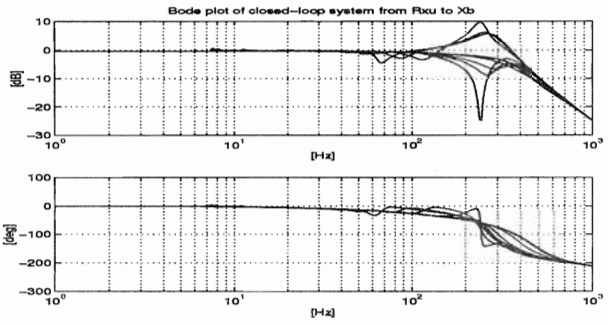

Fig.11 Closed-loop system with GSC
(Output is below side)

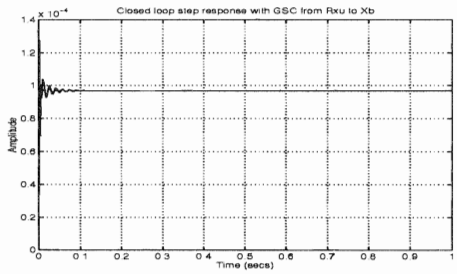

Fig.12 Step response of closed-loop system with GSC
(Output is below side)

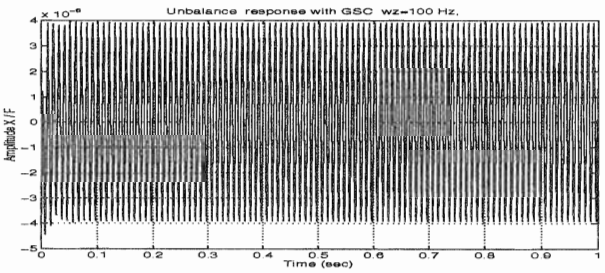

Fig.13 Unbalance time-history response with GSC

6.2 PID Control Results

PID controller is independent of the rotational speed of the rotor. For this reason, the nature of PID controller given in Fig.15 is different from gain-scheduled controller. The bode plots of the closed-loop system with PID control are given in Fig.14 and Fig.17 for different output location. The step responses for upper and below side outputs are shown in Fig.16 and Fig.18, respectively. The time history response of the closed-loop system has big amplitude rate comparing with gain scheduled control(Fig.19).

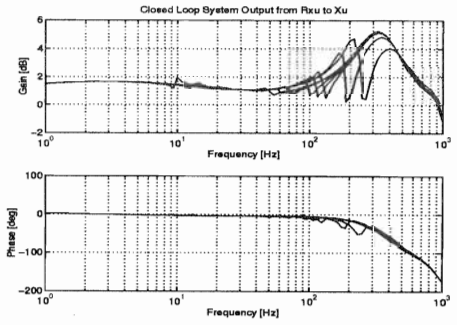

(a)

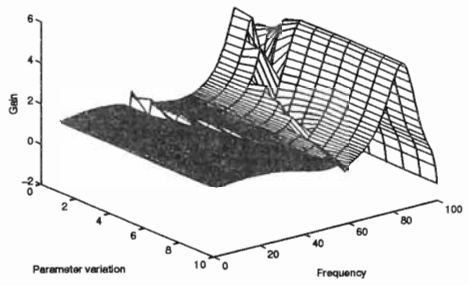

(b)

Fig.14 Bode plot of the closed-loop system with PID
(a) 2D plot (b) 3D plot

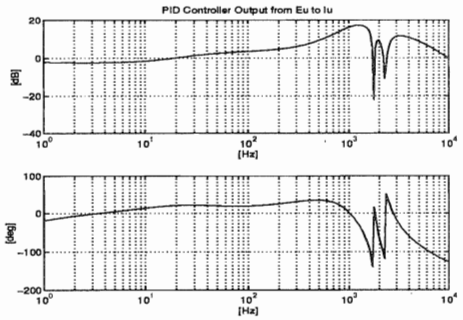

Fig.15 Bode plot of PID controller

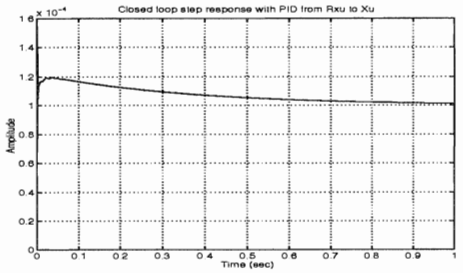

Fig.16 Step response of system with PID

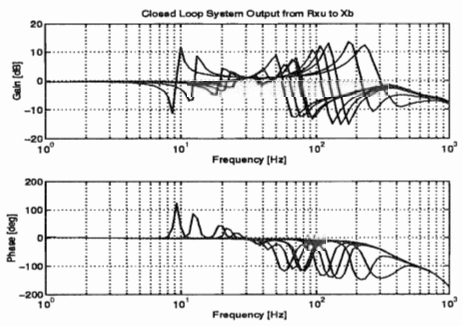

Fig.17 Closed-loop system with PID
(Output is below side)

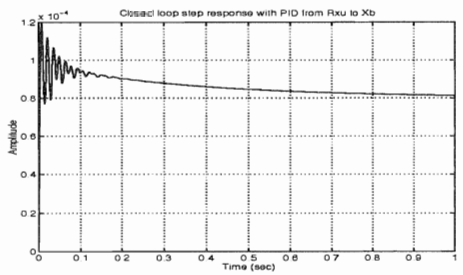

Fig.18 Step response of the system with PID
(Output is below side)

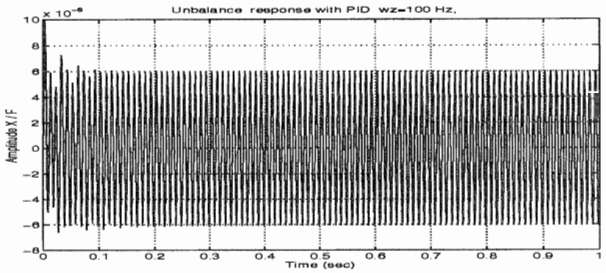

Fig.19 Unbalance time-history response with PID

7 Conclusions

Elimination of gyroscopic effect on a rotor magnetic bearing system is a difficult control task using conventional control techniques because of complex nature of rotor dynamics. Except ideal systems all real systems have unhomegenous structure and this cause unbalance forces in rotating machines even if we perfectly balance the rotating parts. Because of very high operational speed of the rotor, the elimination of unbalance effect is as important as elimination of gyroscopic effect.
In this study, gyroscopic and unbalance disturbance effects of vertically designed an AMB system are eliminated using recently available LMI based gain scheduled H_∞ control. The results obtained here are reasonable and encouraging for future studies on AMB systems. Our aim is to realize this new concept gain scheduled controller experimentally. The planned experimental studies will be carried out using obtained results soon.

References

[1] K. Nonami, T. Ito. μ Synthesis of Flexible Rotor Bearing Systems, IEEE. Trans. on Control Systems Technology, Special Issue on Magnetic Bearings , to appear 1996.

[2] K. Nonami, S. Sivrioglu, H. Ueyama. Active Magnetic Bearing System by Means of LMI Based H_∞ Control and Mixed H_2/H_∞ Control, JSME Journal (Japaneese), to appear 1996.

[3] K. Nonami, H. Ueyama and Y.Segawa. H_∞ Control of Milling Spindle, Proceedings of 4th ISMB, 531-536(1994), ETH Zurih.

[4] F.Matsumura, M.Fujita, K.Hatake, M.Hirai, Elimination of Unbalance Vibration in AMB Systems Using Gain Scheduled H_∞ Robust Controllers, Proceedings of 4th ISMB, 113-118 (1994), ETH Zurih.

[5] P. Apkarian, P. Gahinet, A Convex Characterization of Gain Scheduled H_∞ Controllers, IEEE. Trans. on Automatic Control, 40(1995) 853-863.

[6] P. Apkarian, P. Gahinet, Self-scheduled H_∞ Control of Linear Parameter-varying Systems: a Design Example, Automatica,vol.31-9, pp.1251-1261,1995. 40(1995) 853-863.

[7] P. Gahinet, A. Nemirovski, A.J. Laub, M. Chilali, LMI Control Toolbox, For Use with MATLAB, 1995.